DIGITAL PARTICLE IMAGE VELOCIMETRY USING SPLINES IN TENSION

U. von Toussaint and S. Gori

Max-Planck-Institute for Plasma Physics, Boltzmannstrasse 2, 85748 Garching, Germany

Abstract. Digital particle imaging velocimetry has become a widely used diagnostic technique for the extraction of quantitative information about flow fields. Multiple-view geometries are used to identify and track individual particles (tracers) at discrete times. Often particle velocities and accelerations are subsequently derived by ill-conditioned methods based on finite-differences of the noisy measurements of the particle positions. Here a different Bayesian approach based on a model of the particles in 3-D velocity space using splines in tension is presented, thus automatically including the physical constraints of finite acceleration. The properties of the new algorithm will be compared with the conventional approach and it is argued that the (exponential) spline model should be formulated in the space where the quantity to be modelled is continous, instead of being placed in the data space.

Keywords: Exponential Splines, Particle Image velocimetry, Gradient estimation
PACS: 02.50.Tt, 02.50.Bf, 52.25Tx

INTRODUCTION

The development of Particle Image Velocimetry, a measurement technique which allows for capturing velocity information of particles from high-speed image recordings, has made huge progress in the last two decades. This is mainly due to the transition from photographical recordings to digital recordings which allows a much faster data extraction and data processing while also tremendously increasing the amount of available data. One of the most common experimental set-ups is the interrogation of a sample volume by a combination of several high-speed video cameras (the recording time for individual frames has meanwhile been improved to around 100 ns) observing from different angles. The visibility of tracer particles is often improved by stroboscopic illumination with intense laser light. For a recent review of used techniques and further details see [1]. In subsequent post-processing steps the 2-D recordings are either considered as intensity fields and techniques like flow-field extraction based on FFT-transforms of the recordings are used or individual particles are identified (which severly limits the possible number of tracer particles) and traced over time. For this the extraction of the location of the particles in 3-D-space from the 2-D-images is mandatory. This is one of the basic problems of computer vision [2] and well studied - although in practice still challenging. However, the algorithms are optimized with respect to the position in space. Far less attention has been given to the proper extraction of velocities and accelerations from the recordings. Even in Particle Image Velocimetry(!) the velocity is often derived by finite differencing of the noisy estimates of the spatial locations (see e.g. [1],

chapter 6 and references therein) - which results in huge estimation uncertainties. Other approaches are based on fitting some smoothing regression function to the noisy spatial data (e.g. cubic splines) [3] with subsequent analytic differentation of the regression function. This method is much more stable than the first one - but results in a systematic underestimation of the differential quantities due to the smoothing in data space. This has been noted by several authors, see e.g. [4]. Subsequently regression functions were suggested which also incorporated the possibility for non-smooth regression. However, applied to the case of Particle Image Velocimetry (PIV) analysis of mock data still revealed systematic deviations, especially for the estimated acceleration. It is argued that the discrepency is due to the omission of known constraints: The force acting on particles is always finite, thus resulting in a possibly non-differentiable but continous velocity profile. Therefore the trace in 3-D space has at least one continous derivative and this has to be taken into account for a consistent estimation of velocity and accelerations.

ESTIMATION OF 3-D POSITION

The estimation of the 3D-position of particles can be divided into three steps: camera calibration, point matching and refined 3D position calculation.

Camera Calibration

Simple camera model are often based on idealized imaging systems as e.g. the well-known pinhole imaging model. The cameras can be calibrated (determination of relative position and orientation) either using calibration targets or using a number of at least 7 point matches (since the fundamental matrix has 7 degrees of freedom) in two different views. For a distortion-free imaging system a direct linear transformation between object and image space yields

$$\begin{bmatrix} u_i w_i \\ v_i w_i \\ w_i \end{bmatrix} = \begin{bmatrix} a_{11} & a_{12} & a_{13} & a_{14} \\ a_{21} & a_{22} & a_{23} & a_{24} \\ a_{31} & a_{32} & a_{33} & a_{34} \end{bmatrix} \times \begin{bmatrix} x_i \\ y_i \\ z_i \\ 1 \end{bmatrix} \tag{1}$$

The parameters $a_{11}, \ldots, a_{34}$ can e.g. be determined by minimizing the distance between the observed $\{u, v\}$ (scaled by a common factor w) pixel coordinates and the computed ones for a set of corresponding 3-D points. It should be pointed out that in practice often more complex imaging models than the pinhole imaging model are necessary to describe the optical transfer function [5].

Point Matching

In the point pair matching stage, the epipolar geometry is used to find the one-to-one relationships between groups of points in the images of the different cameras.

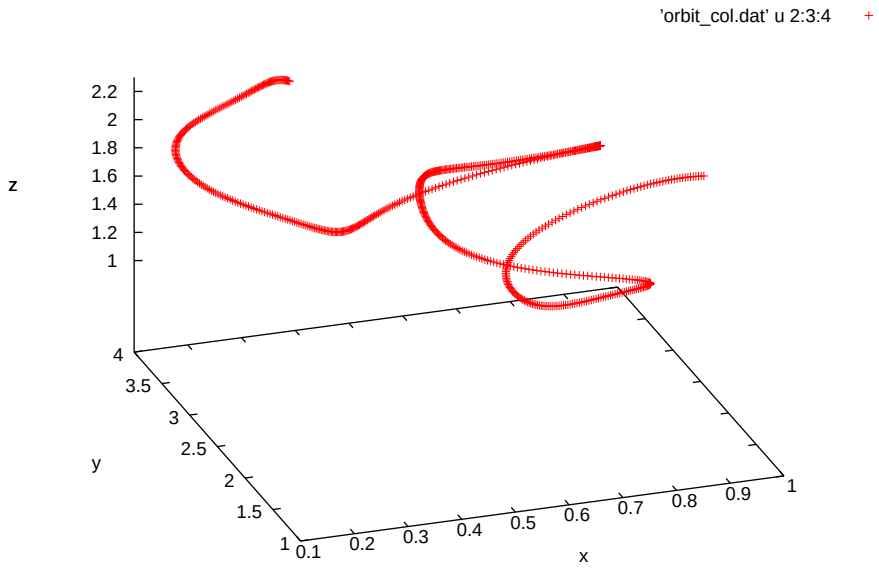

FIGURE 1. Simulated 3-D trajectorie of a charged particle injected into a fusion device with electrical and magnetic fields acting on it

Corresponding points lie on the respective epipolar lines in different views [6], which can be exploited to reduce the matching problems to efficient 1-D line searches. For more details on that topic see any textbook about computer vision, e.g. [6]

3D Coordinate Calculation

Based on the image coordinates of corresponding points (with limited resolution due to a finite pixel size) the probability distribution of the location in space can be derived $p(x,y,z \mid u,v,t_i,I)$ (e.g. by back-projection), which is often approximated by a three-dimensional Gaussian distribution. Here additional information like the intensity of adjacent image pixels can be used to improve the accuracy of the position estimation.

For every frame recorded at time t_i the individual probability distributions of the particles are then available. The task is to infer the trajectories, velocities and accelerations of the individual particles. A typical example of a trajectorie of a charged particle in a fusion device is shown in Fig.1. Please note how phases of a relative smooth movement alternate with abrupt direction changes. Typically only a few particles are observed in each video frame. Therefore, unlike e.g. in many hydrodynamic settings, correlations and interactions between the particles are only rarely observed and thus presently not taken into account but could in principle (on the expense of a much more complicated model) be included.

SPLINES IN TENSION

Splines in tension, also known as exponential splines have been studied by several authors, see e.g. [7, 8, 9, 4], therefore we give only a brief description of the main properties. The exponential spline is the solution of a minimal bending energy functional

$$\int_{x_0}^{x_N} \mathrm{d}x \left\{ \left(\frac{\mathrm{d}^2 \mathrm{S}(x)}{\mathrm{d}x^2} \right)^2 + \lambda(x)^2 \left(\frac{\mathrm{dS}(x)}{\mathrm{d}x} \right)^2 \right\} \tag{2}$$

with $S(\xi_i) = f_i, i = 0, \ldots, N$ and

$$\lambda(\xi) = \lambda_i \text{ for } \xi_i \leq x \leq \xi_{i+1}, i = 0, \ldots, N-1. \tag{3}$$

$\lambda(x)$ is proportional to the tensile forces in each interval. For vanishing λ_i this functional has a minimum if $S(x)$ is a cubic spline. If on the other hand λ_i tends to infinity the functional is minimized by a picewise linear function. Therefore splines in tension may be considered as ideal representation of the physical properties of the velocity of particles in force fields: Capable of accomodation of short impulses if required by the data but otherwise 'prefering' a constant acceleration (force).

The variational problem of Equation 2 can be recasted as Euler-Lagrange equation

$$\left\{ \frac{\delta^4}{\delta x^4} - \lambda_i^2 \frac{\delta^2}{\delta x^2} \right\} S(x) = 0 \text{ for } \xi_i \leq x \leq \xi_{i+1}. \tag{4}$$

The solution is given by the fundamental system $\{1, x, \exp(\lambda_i x), \exp(-\lambda_i x)\}$, whose numerical properties, however, are ill-behaved for $\lambda_i \to 0$ and $\lambda_i \to \infty$. In [10, 9] a reformulation is given which is numerically more convenient:

$$S(x) = f_{i+1}h + f_i(1-h) + \frac{M_{i+1}}{\lambda_i^2}\left(\frac{\sinh(\mu_i h)}{\sinh \mu_i} - h \right) + \frac{M_i}{\lambda_i^2}\left(\frac{\sinh(\mu_i(1-h))}{\sinh \mu_i} - (1-h) \right), \tag{5}$$

with the function values f_i given at the support points ξ_i, M_i the second derivative of $S(x)$ at the support point ξ_i and the following definitions:

$$h = \frac{x - \xi_i}{\xi_{i+1} - \xi_i} \text{ and } \mu_i = \lambda_i(\xi_{i+1} - \xi_i), i = 0, \ldots, N-1. \tag{6}$$

The unknown values of the second derivatives $\{M_i\}$ can be determined from the continuity requirement of the first derivative, yielding a symmetric, positive definite tridiagonal system for the second derivatives which can be solved efficiently. With this solution the spline can be expressed as matrix-vector multiplication of the design matrix (depending on the location of the data points $\vec{x}$, the x-locations of the support points $\vec{\xi}$ and the corresponding vector of tension parameters $\vec{\lambda}$) with the vector of function values $\vec{f}\left(\vec{\xi}\right)$ [11]

$$S(\vec{x}) = \mathbf{W}\left(\vec{x}, \vec{\lambda}, \vec{\xi}\right) \vec{f}\left(\vec{\xi}\right). \tag{7}$$

The integral

$$T(x_1) = \left(\int_{x_0}^{x_1} \mathrm{d}x \vec{W}\left(x_1, \vec{\lambda}, \vec{\xi}\right) \right) \vec{f}\left(\vec{\xi}\right), \tag{8}$$

can also be calculated analytically (please note: here shown for a single value x_1 instead of the full vector $\vec{x}$ to keep the notation simple) speeding up the numerical optimizations.

THE BAYESIAN FRAMEWORK

With the prior expectation that splines in tension are an adequate description of the particle *velocity*, the basic idea is to match the data points with the spline values integrated over time.

From here the independent variable is time (the recording time of the frames), differing from the previous sections where x was used as the independent variable to be in agreement with standard literature.

The likelihood distribution

The data analyzed in the present work are the 3-D coordinate estimates $\vec{r}_j = \left(x_j, y_j, z_j\right)^T$ at time t_j derived from the multi-view camera system together with the associated 3×3-covariance matrix $\mathbf{C}_j$ which yields the multivariate Gaussian likelihood

$$p\left(\vec{r}_j \mid \mathbf{C}_j, t_j, \vec{f}_{\vec{r}}, \vec{\lambda}_{\vec{r}}, \vec{\xi}_{\vec{r}}, \vec{r}_0, I\right) = \sqrt{\det\left(\mathbf{C}_j^{-1}/2\pi\right)} \cdot \exp\left[-\frac{1}{2}\left(\vec{r}_j - \left(\mathbf{T}_{\vec{r}j} + \vec{r}_0\right)\right)^T \mathbf{C}_j^{-1}\left(\vec{r}_j - \left(\mathbf{T}_{\vec{r}j} + \vec{r}_0\right)\right)\right], \tag{9}$$

where the subscript $\vec{r}$ is used to indicate the three cartesian components: $\mathbf{T}_{\vec{r}j} = \left(\mathbf{T}_{xj}, \mathbf{T}_{yj}, \mathbf{T}_{zj}\right)^T$. Every component is described by its own independent spline function, which are only coupled via the likelihood covariance matrix and the common independent time variable $\vec{t}$, i.e. the number and position of support points may be different, thus accomodating trajectories with different behaviour in the respective directions (e.g gyromotion due to Lorentz-forces). In other circumstances a different parametrization may be adequate, e.g. a pseudo-arclength parametrization which introduces a stronger coupling between the individual components.

The prior probability distributions

The computation of the posterior requires the specification of the likelihood distribution (see Eq.9) and the prior distributions. The tension parameter $\vec{\lambda}_{\vec{r}}$ is a positive scale

parameter, therefore Jeffrey's prior has been chosen

$$p\left(\vec{\lambda}_{\vec{r}} \mid E_{\vec{r}}, I\right) = \left(\prod_{j=1}^{E_x-1} \frac{1}{\lambda_{xj}}\right)\left(\prod_{j=1}^{E_y-1} \frac{1}{\lambda_{yj}}\right)\left(\prod_{j=1}^{E_z-1} \frac{1}{\lambda_{zj}}\right) \tag{10}$$

with $E_{\vec{r}}$ the total number of support points and $p\left(E_{\vec{r}} \mid I\right) = 1/c$ for sensible values of E_x, E_y, E_z, - every component has at least two support points and none of the components has more than the number of frames. The prior for the velocity amplitudes has been chosen to be constant. The prior for the initial position $\vec{r}_0$ of the particle is zero for any position outside of the observation volume and constant inside. Finally the position of the support points $\xi_{\vec{r}}\left(\vec{t}\right)$ is constraint in such a way that between any two support points there is always at least one data point and that the minimum distance between two neighboured support point is always larger than a minimum distance $\Delta t_{\min}$.

Computation

The ultimate goal is an evaluation of the recordings fast enough to be able to influence the trajectories of the particles, e.g to avoid impact on or near sensitive devices. This long-term goal prevents the use of MCMC methods for a full Bayesian model averaging approach to estimate the velocity and acceleration of the particles. Instead MAP estimates are used, together with the corresponding numerical estimates of the covariance matrices for different number of support points - all of which can be computed in parallel.

RESULTS

In Figure 2 the spatial x-component of the 3-D trajectory displayed in Figure 1 is shown as function of time as dotted line. Using this as ground truth a set of 29 equidistant observations has been simulated by adding Gaussian distributed noise with mean=0 and a standard deviation of $\sigma = 0.03$, shown as filled circles with error bars representing ± 1 standard deviation. In addition the integrated values of the best-fit velocity-space based exponential spline are shown as dashed line. It can be seen that the dashed line follows the underlying trajectory on average more closely than the exponential spline which has been computed using the noisy data-points directly (solid line), although the latter approximates the mock data better. Both exponential splines have the same number of support points.

The difference between the two approaches is more pronounced in the estimated velocities, displayed in Figure 3, upper panel. The solid line represents the true underlying velocity profile (x-component only), which is compared with the derivative of the exponential spline fitting the data directly and with the exponential spline in the velocity space. The larger deviations of the former spline from the true profile are obvious. The latter is generally following the velocity profile quite accurately, with minor deviations at around $t = 3.5$. Comparison with the noisy data in Figure 2 reveals that a slightly lower velocity than the ground truth is in good agreement with the observations. Additionally

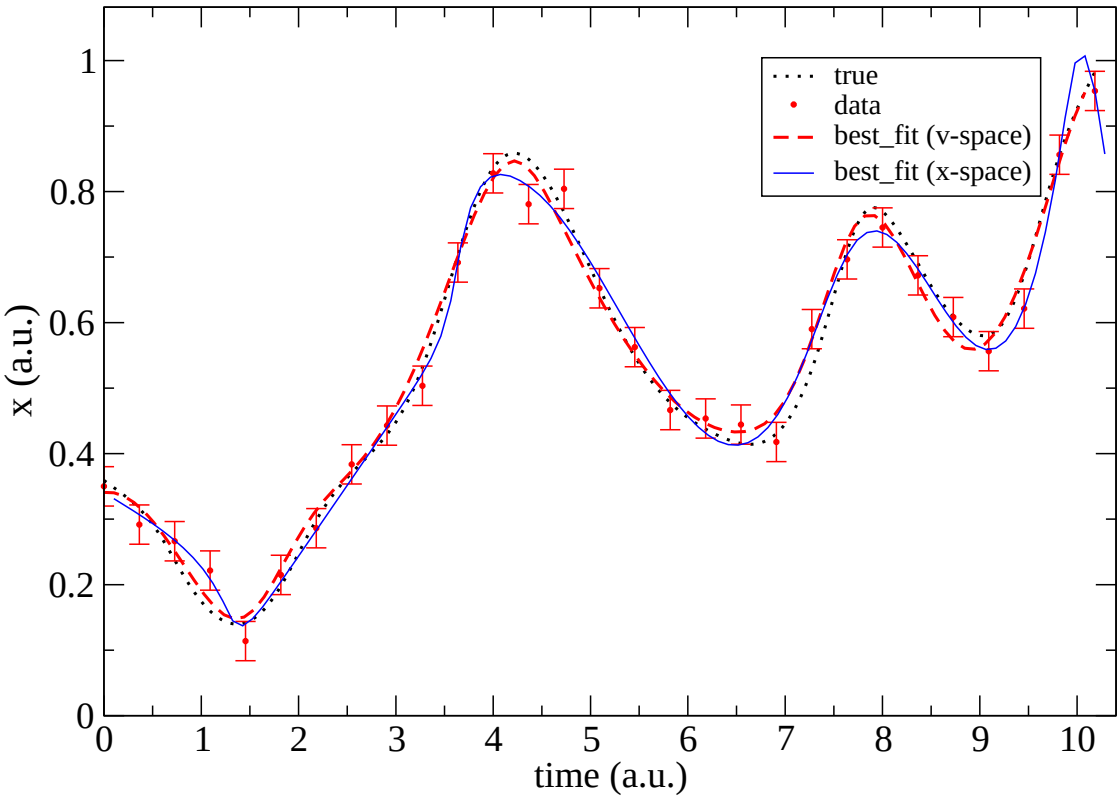

FIGURE 2. Comparison of the spatial x-component of the true trajectory (dotted line) as function of time with estimates based on a direct fit of the noisy data (circles with error bars) with exponential splines (solid line) and with the exponential spline in velocity space (dashed line). The noisy data are better approximated by the directly fitting exponential spline whereas the true trajectory is more closely followed by the exponential spline modelled in velocity space.

the results of a simple finite-differencing scheme are superimposed. The amplification of the noise level is obvious (see e.g. $t = 4$) and the particle acceleration is inaccessible by this approach. The computation of the acceleration by analytic differentation of the exponential splines, however, is possible and is displayed in Figure 3, lower panel. Here the difference between the two splines approaches is already so large that a meaningful interpretation in terms of potentially acting forces is only possible for the velocity-based spline.

Of interest is also the uncertainty of the derived velocity- and acceleration profiles. An efficient and fast way to assess the correlated uncertainties offers the generation of sample trajectories based on the estimated covariance matrix. Using a Cholesky-decomposition of this matrix the necessary multivariate random samples are straightforward to generate. The superimposed samples provide a very informative picture of the uncertainty of the respective estimates (not shown).

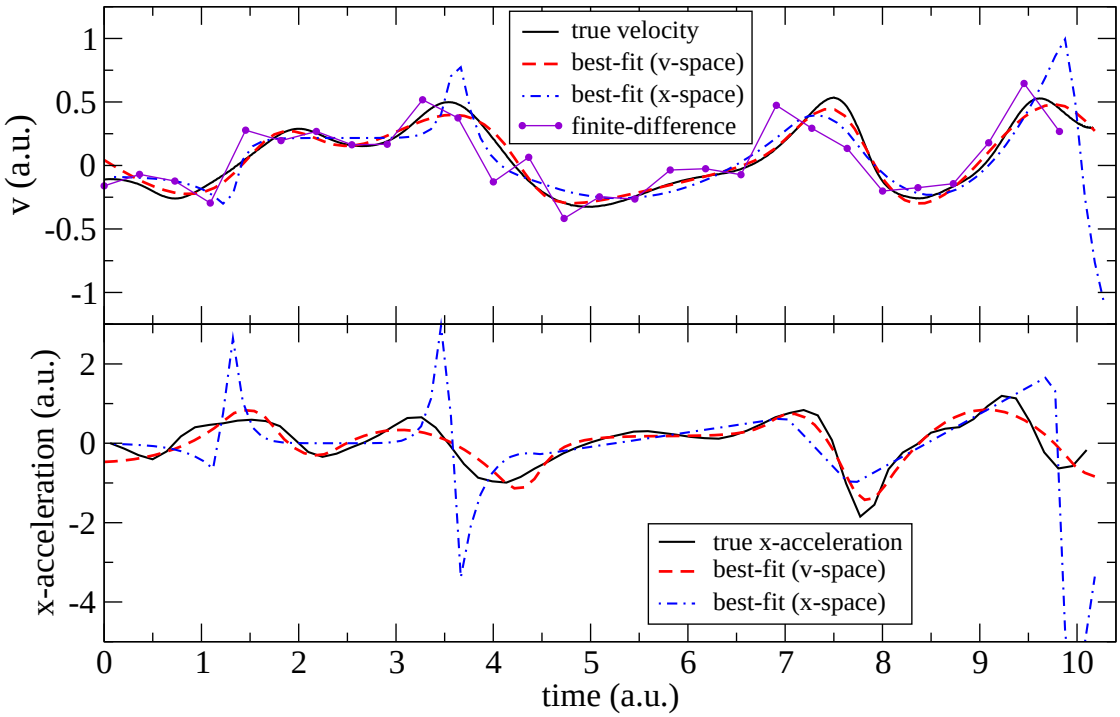

FIGURE 3. Upper panel:Comparison of the x-component of the velocity v_x (solid line) of the true trajectory with estimates based on a direct fit of the noisy data with exponential splines (dashed-dotted line) and with the exponential spline in velocity space (dashed line). The v_x estimation by the velocity-space based spline is closely resembling the ground truth. In addition the result of a finite-differencing scheme of the noisy data is displayed (solid circles, connected with lines). Lower panel: Comparison of the x-component of the acceleration a_x (solid line) of the true trajectory with estimates based on a direct fit of the noisy data with exponential splines (dashed-dotted line) and with the exponential spline in velocity space (dashed line). The a_x estimation by the velocity-space based spline does not exhibit the spiky structure of the direct fitting spline and is thus a much more reliable estimator of the acting forces.

CONCLUSION AND OUTLOOK

Using realistic simulation data of charged particles in fusion devices, it has been shown that a description of particle trajectories by splines in tension in *velocity space* is superior to approaches solely based in the data-space (the present state of art) if velocities and forces (accelerations) are of interest. The next steps are the extension of the forward model (mapping of the spline onto the pixel coordinates of the recording cameras to circumvent the intermediate step of an 3-D position estimation of the particle) followed by predictive modelling and improved post-processing (=off-line) analysis using MCMC for Bayesian model averaging. The exploitation of the idea of separating the space where the modelling spline resides from the observed (data) space promises to be beneficial also for other situations where derivatives of measured quantities are required, e.g. for Langmuir probe measurements or in robot control.

ACKNOWLEDGMENTS

The authors would like to acknowledge the helpful and informative discussions with V. Rohde and N. Endstrasser about the properties and sources of particles in tokamaks.

REFERENCES

1. M. Raffel, C. Willert, S. Wereley, and J. Kompenhans, *Particle Image Velocimetry*, Springer, Berlin, 2007.
2. R. Hartley, and A. Zisserman, *Multiple View Geometry in Computer Vision*, Cambridge University Press, Cambridge, 2004.
3. W. H. Press, S. A. Teukolsky, W. T. Vetterlin, and B. P. Flannery, *Numerical Recipes in Fortran 90*, Cambridge University Press, Cambridge, 1996.
4. V. Dose, and R. Fischer, "Function estimation employing exponential splines," in *Bayesian Inference and Maximum Entropy Methods in Science and Engineering*, edited by K. Knuth, A. Abbas, R. Morris, and J. Castle, AIP Conference Proceedings 803, American Institute of Physics, Melville,New York, 2005, pp. 67–71.
5. B. Wieneke, *Exp. Fluids* **39**, 267–2280 (2005).
6. Y. Ma, S. Soatto, J. Kosecka, and S. S. Sastry, *An Invitation to 3-D Vision*, Springer, New York, 2003.
7. S. Pruess, *J. Approximation Theory* **17**, 86–96 (1976).
8. D. G. Schweikert, *J. Math. Phys.* **45**, 312–317 (1966).
9. P. Rentrop, *Numer. Math.* **35**, 81–93 (1980).
10. A. Cline, *Comm. ACM.* **17**, 218–223 (1974).
11. R. Fischer, and V. Dose, "Flexible and reliable profile estimation using exponential splines," in *Bayesian Inference and Maximum Entropy Methods in Science and Engineering*, edited by A. Mohammad-Djafari, AIP Conference Proceedings 872, American Institute of Physics, Melville,New York, 2006, pp. 296–303.